

Intrinsic Branching Effects in Syndiotactic Copolymers of Propylene and Higher α -Olefins

Eric D. Schwerdtfeger and Stephen A. Miller*

Department of Chemistry, Texas A&M University, College Station, Texas 77843-3255

Received January 9, 2007; Revised Manuscript Received May 21, 2007

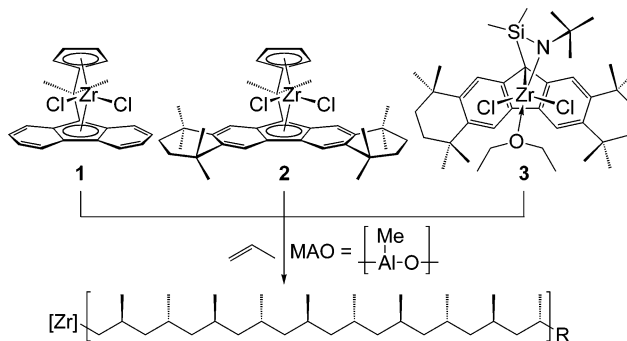
ABSTRACT: Copolymers of propylene with higher α -olefins (4-methyl-1-pentene, 1-hexene, 1-octene, and 1-decene) have been synthesized at 0 °C using the syndiospecific catalysts $\text{Me}_2\text{C}(\eta^5\text{-C}_5\text{H}_4)(\eta^5\text{-C}_{13}\text{H}_8)\text{ZrCl}_2$ (**1**), $\text{Me}_2\text{C}(\eta^5\text{-C}_5\text{H}_4)(\eta^5\text{-C}_{29}\text{H}_{36})\text{ZrCl}_2$ (**2**), and $\text{Me}_2\text{Si}(\eta^1\text{-C}_{29}\text{H}_{36})(\eta^1\text{-N-}t\text{Bu})\text{ZrCl}_2\cdot\text{OEt}_2$ (**3**) activated with methylaluminoxane (MAO). For each catalyst, the observed melting temperature (T_m) depression of the syndiotactic copolymers was found to be linearly dependent on the molar fraction of comonomer incorporated, but little dependence on the identity of the comonomer was detected. The observed *rmrr* stereochemical pentad fraction present in the copolymers was proportional to the mol % of comonomer incorporation, suggesting that each comonomer insertion induces an average of 1.2 site epimerization stereoerrors for the three catalysts operating at 0 °C. The catalyst **3**/MAO produced the fewest enantiofacial misinsertions and the copolymers with the highest melting temperatures for any given incorporation of comonomer. The unequal syndiospecificity of **3**/MAO has made it possible to more accurately measure the intrinsic effect of branches on the melting temperature of syndiotactic copoly[propylene/higher α -olefin]. The best fit linear relationship was found to be $T_m = 161.7\text{ °C} - 7.6\text{ °C}(\text{mol \% comonomer})$.

Introduction

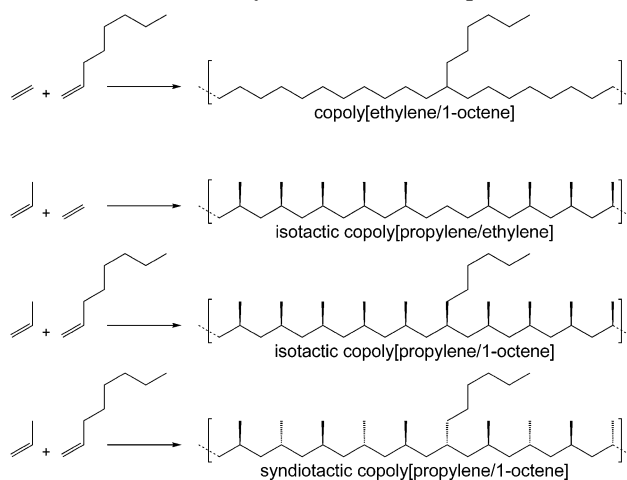
The 1988 report by Ewen, Razavi, et al. was the first to describe the preparation of syndiotactic polypropylene (*s*-PP) using a single-site catalyst. The polymer produced by the C_s -symmetric *ansa* metallocene $\text{Me}_2\text{C}(\eta^5\text{-C}_5\text{H}_4)(\eta^5\text{-C}_{13}\text{H}_8)\text{ZrCl}_2$ (**1**)—in combination with methylaluminoxane (MAO) cocatalyst—was crystalline, with a T_m (melting temperature) of 138 °C and a syndiotactic pentad fraction of $[rrrr] = 86\%$ (Scheme 1).¹ Global commercial production of *s*-PP relies completely on single-site catalysts and has reached a capacity of ~ 14 million kg/year.² One forecast for the annual production of 400 million kg by 2010³ is likely overestimated but does reflect much of the optimism held for this polymer and its niche markets.⁴ Improvements in syndiospecific catalytic systems have included doubly bridged metallocenes,⁵ nonmetallocenes,⁶ and sterically expanded derivatives of the parent Ewen–Razavi catalyst, such as $\text{Me}_2\text{C}(\eta^5\text{-C}_5\text{H}_4)(\eta^5\text{-C}_{29}\text{H}_{36})\text{ZrCl}_2$ (**2**).⁷ Catalyst **2**/MAO is capable of producing *s*-PP with a higher $[rrrr]$ (92%) and T_m (154 °C). Additional increases in $[rrrr]$ and T_m have recently been reported using the easily synthesized, sterically expanded constrained geometry catalyst (CGC) $\text{Me}_2\text{Si}(\eta^1\text{-C}_{29}\text{H}_{36})(\eta^1\text{-N-}t\text{Bu})\text{ZrCl}_2\cdot\text{OEt}_2$ (**3**).^{8,9} Catalyst **3**/MAO produces *s*-PP with $[rrrr] > 99\%$ and $T_m = 165\text{ °C}$; the annealed *s*-PP polymer melts at 174 °C.¹⁰

Comonomer Strategy. The crystallinity of polyolefins, along with other fundamental properties, can be greatly affected by even small amounts of short-chain or long-chain branching.¹¹ Commercial linear low-density polyethylene (LLDPE), produced by copolymerizing ethylene with α -olefins using classical heterogeneous catalysts¹² or constrained geometry catalysts,¹³ is a noteworthy example. The mechanical properties of LLDPE can be finely modulated by controlling the amount of incorporated comonomer, which is typically 1–4 mol %, but can be as high as 25 mol % for low-crystallinity plastomers.¹¹ This

Scheme 1. Single-Site Catalysts 1, 2, and 3 for Producing Syndiotactic Homopolypropylene



Scheme 2. Comonomer Strategy Disrupts Crystallinity and Modulates Polymer Mechanical Properties



comonomer strategy (Scheme 2), which controllably disrupts crystallinity, is most commonly exploited to vary the properties of polyethylene, but it has also given rise to an array of isotactic polypropylene copolymers with controlled comonomer incorporation (albeit ethylene is often the comonomer). However,

* To whom correspondence should be addressed. E-mail: samiller@mail.chem.tamu.edu.

Table 1. Propylene/Comonomer Copolymerization Results with 1, 2, and 3 (Activated with MAO)^a

entry	comonomer	comonomer (mL)	comonomer feed fraction (mol %)	comonomer incorporation (mol %)	activity ^b	<i>T</i> _m (°C)	[<i>rrrr</i>] (%)	[<i>rmrr</i>] (%) ^c	[<i>rrmm</i>] (%)
Catalyst 1/MAO									
1 ^d	none				2400	151.4	91.4	1.0	1.0
2	4-methyl-1-pentene	1.0	2.5	1.1	3650	138.4	87.1	3.6	1.2
3	4-methyl-1-pentene	3.0	7.6	3.0	2860	118.8	81.2	6.8	1.1
4	4-methyl-1-pentene	5.0	13.2	8.5	4690	am	72.2	11.4	1.0
5	4-methyl-1-pentene	5.0	13.2	8.0	3900	am	74.3	11.3	0.6
6	4-methyl-1-pentene	10.0	28.8	17.8	5060	am	48.2	23.8	0.8
7	1-hexene	1.0	2.5	0.8	2340	134.0	87.5	3.4	1.1
8	1-hexene	3.0	7.8	5.0	2990	103.5	74.0	10.7	0.9
9	1-hexene	5.0	13.5	8.9	4100	am	64.6	15.5	0.9
10	1-hexene	10.0	29.3	19.8	5400	am	37.3	27.6	1.5
11	1-octene	1.0	2.0	1.7	3380	135.2	91.2	2.3	0.8
12	1-octene	1.0	2.0	1.4	940	132.5	91.0	2.7	0.7
13	1-octene	3.0	6.3	4.6	6360	101.2	79.7	8.7	0.6
14	1-octene	5.0	11.0	10.0	4060	am	69.9	13.0	0.8
15	1-octene	20.0	24.7	12.1	650	am	37.2	26.0	2.2
16	1-decene	1.0	1.7	1.2	650	141.0	84.9	3.4	1.6
17	1-decene	3.0	5.3	4.3	1830	108.8	82.4	7.1	0.7
18	1-decene	5.0	9.3	9.3	3970	am	67.1	13.1	1.4
Catalyst 2/MAO									
19 ^d	none				1830	157.3	95.6	1.6	0.0
20	4-methyl-1-pentene	1.0	2.5	1.0	520	150.1	95.7	1.7	0.2
21	4-methyl-1-pentene	3.0	7.6	2.7	340	129.2	85.6	6.1	0.5
22	4-methyl-1-pentene	5.0	13.2	4.4	310	114.6	83.1	8.1	0.1
23	4-methyl-1-pentene	10.0	28.8	10.1	40	am	76.5	11.4	0.1
24	1-hexene	1.0	2.5	2.0	830	139.0	92.2	2.9	0.4
25	1-hexene	3.0	7.8	4.1	1590	113.4	82.8	7.1	0.6
26	1-hexene	5.0	13.5	5.8	1000	102.1	70.5	14.6	0.1
27	1-hexene	10.0	29.3	14.1	490	am	49.9	22.0	1.2
28	1-octene	1.0	2.0	0.9	620	141.5	91.9	3.6	0.2
29	1-octene	1.0	2.0	1.4	380	139.8	81.7	7.3	0.7
30	1-octene	3.0	6.3	3.1	880	117.0	85.8	6.1	0.4
31	1-octene	5.0	11.0	7.4	580	101.9	74.6	11.4	0.5
32	1-octene	10.0	24.7	15.1	620	am	53.4	20.8	1.0
33	1-decene	1.0	1.7	0.9	350	142.7	93.5	2.7	0.2
34	1-decene	3.0	5.3	3.7	530	113.5	86.5	6.3	0.2
35	1-decene	5.0	9.3	6.7	520	97.8	74.0	11.6	0.6
Catalyst 3/MAO									
36 ^d	none				3890	163.6	97.6	1.1	0.0
37	4-methyl-1-pentene	1.0	2.5	1.3	2490	153.1	94.4	2.1	0.3
38	4-methyl-1-pentene	2.0	5.0	2.8	2770	142.8	90.2	4.3	0.2
39	4-methyl-1-pentene	3.0	7.6	3.7	290	139.1	88.7	5.1	0.2
40	4-methyl-1-pentene	5.0	13.2	6.5	890	120.2	77.4	10.3	0.4
41	4-methyl-1-pentene	10.0	28.8	15.8	670	am	64.7	15.6	0.8
42	1-hexene	1.0	2.5	2.5	130	149.8	90.9	3.8	0.3
43	1-hexene	3.0	7.8	4.8	580	121.6	83.4	7.7	0.2
44	1-hexene	5.0	13.5	8.6	570	101.3	68.0	14.6	0.5
45	1-hexene	5.0	13.5	8.6	190	92.8	66.6	16.4	0.1
46	1-hexene	10.0	29.3	20.9	830	am	37.0	28.5	1.2
47	1-octene	1.0	2.0	1.0	1240	149.1	93.7	2.8	0.2
48	1-octene	3.0	6.3	4.3	1320	123.3	81.1	8.9	0.2
49	1-octene	5.0	11.0	7.4	670	102.3	72.6	12.5	0.5
50	1-octene	10.0	24.7	17.1	1020	am	48.4	22.7	1.3
51	1-decene	1.0	1.7	1.2	1410	150.8	95.1	1.9	0.2
52	1-decene	3.0	5.3	4.1	1890	125.8	83.1	7.7	0.3
53	1-decene	5.0	9.3	5.6	1560	116.6	78.2	9.8	0.4

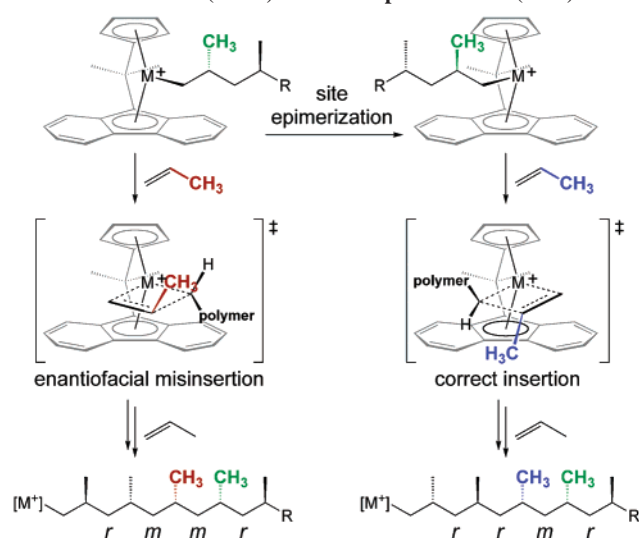
^a Polymerization conditions: propylene/comonomer solution (25 mL); 1000 equiv of MAO; 0 °C; 2 min runs except entry 2 (10 min), entry 3 (3 min), entry 4 (4 min), entries 1, 19, 36, 37, 38, and 39 (5 min), and entry 41 (2.5 min). ^b In kg of polymer/(mol of Zr h). ^c Since [*rrmm*] is likely negligible, [*rmrr*] ≈ [*rmrr*] + [*rrmm*]. ^d Data from ref 10.

there are no current commercial examples that exploit this tactic to create a series of *syndiotactic* polypropylene copolymers.

Tactic Copolymers. Because of massive worldwide production of isotactic polypropylene (over 40 billion kg/year)¹⁴ and the tunability of isoselective catalysts, the relationships between microstructure and polymer properties have been well studied for *i*-PP.^{15–19} Recent works by Hiltner,²⁰ De Rosa,²¹ and Lotz²² have indicated that incorporation of small amounts of higher α -olefins into isotactic polypropylene samples can cause a sharp decrease in the melting temperature of the samples due to exclusion of the longer chains from the crystal lattice. At higher

incorporations between 10 and 25 mol %, however, the decrease in *T*_m becomes more gradual, as the crystal structure changes to one isomorphous with that of isotactic poly(1-butene). This crystal structure allows the side chains to be included within the crystal lattice, and the polymer samples can therefore remain highly crystalline, with melting temperatures similar to that of isotactic poly(1-butene).

The marginal commercial importance and greater synthetic challenges of *s*-PP have resulted in relatively few copolymers based on syndiotactic polypropylene. Crystallization phenomena have been investigated for samples of *s*-poly[propylene/1-

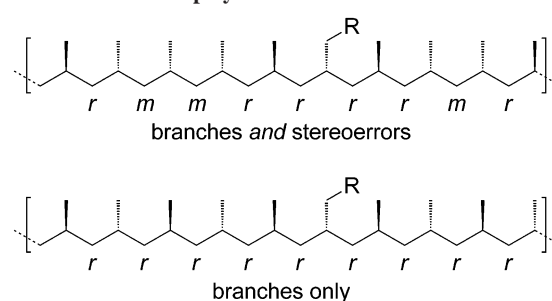
Scheme 3. Stereochemical Consequences of Enantiofacial Misinsertion (*rmmr*) and Site Epimerization (*rmr*)

butene],^{23–25} *s*-poly[propylene/1-hexene],^{26–28} and *s*-poly[propylene/1-octene],^{29–32} but a literature survey reveals several emergent themes. (1) Because these investigations employ the commercially available Ewen–Razavi catalyst (**1**), the level of syndiotacticity in the obtained copolymers is usually limited to $[r] \approx 90\%$. (2) Most reports do not disclose details about the stereoerrors present in the copolymers. Therefore, the effects of these stereoerrors and the effects of the branches remain commingled. (3) These reports offer few, if any, details about the actual polymer synthesis. Catalyst behavior is typically neglected when stock samples of *s*-PP are employed. (4) The mechanical properties of these copolymers remain largely unexplored. A report from 1995 did disclose a decreasing tensile modulus with increasing 1-octene incorporation, as expected.²⁹

Graef and co-workers²⁷ reported that incorporation of an α -olefinic comonomer into syndiotactic polypropylene produced using the Ewen–Razavi catalyst (**1**) causes the T_m of the copolymers to decrease linearly with increasing comonomer incorporation; this effect does not depend on the identity of the α -olefin comonomer (e.g., 1-hexene, 1-dodecene, 1-octadecene), only on the molar fraction of comonomer that is incorporated. They suggest that the observed effect might be partially due to a decrease in stereoregularity rather than being entirely a result of crystal lattice disruption caused by the side chains (e.g., *n*-butyl, *n*-decyl, *n*-hexadecyl) appended to the polymer chain. The *rmrr* pentad fraction increased as comonomer incorporation increased, suggesting that the higher α -olefins effected an increase in site epimerization (Scheme 3),^{18,33,34} typically the major source of stereoerrors produced by syndiospecific olefin polymerization catalysts. The linear relationship, computed for 34 samples prepared at 20 °C with **1**/MAO, is given by $\%[\text{rmrr}] = 2.6 + 2.3(\text{mol } \%$ comonomer). Under these conditions, each incorporated comonomer apparently induces 2.3 additional site epimerization events. The other principal source of stereoerrors is enantiofacial misinsertion, which gives rise to the *rmmr* stereoerror pentad (Scheme 3).^{7,18} According to Graef et al., this type of error does not correlate to the mol % of comonomer incorporated with **1**/MAO at 20 °C but is found to range between 0.7% and 2.0%, with an average of 0.9%.²⁷

We have extended the work of Graef et al. to include different comonomers at higher incorporations using the markedly more syndiospecific catalysts **2** and **3**. Additionally, we performed polymerizations at 0 °C (vs 20 °C) in order to increase the syndiospecificity of the catalysts while retaining reasonable polymerization activities.¹⁰ Because of the enhanced stereose-

Scheme 4. An Ideal Assessment of Branching Effects Should Be Performed on Copolymers with Minimal Stereoerrors



lectivity of the selected catalysts, we anticipated that highly syndiotactic copolymers would be obtained and that the variance in the copolymer melting temperature would more truly reveal the *intrinsic effect of the incorporated branches*, not the combined effect of branches and stereoerrors, as are abundantly found with the parent Ewen–Razavi catalyst, **1** (Scheme 4).

Results and Discussion

Copolymer Synthesis and Characterization. A series of copolymers was synthesized in liquid propylene/comonomer at 0 °C, as detailed in Table 1. Polymerization conversion was purposefully kept low ($\leq 5\%$) so that a constant propylene/comonomer quotient could be assumed. The comonomers employed were 4-methyl-1-pentene, 1-hexene, 1-octene, and 1-decene, and the comonomer feed fraction ranged from 0 to 30 mol %. Each polymer sample was analyzed by ¹³C NMR spectroscopy to determine the stereochemical pentad distribution and, especially, the abundances of the *rmrr* stereoerror pentad (site epimerization) and the *rmmr* stereoerror pentad (enantiofacial misinsertion). The ¹³C NMR spectra also indicated the percent incorporation of comonomer. Additionally, differential scanning calorimetry (DSC) was performed to ascertain melting temperatures of the copolymer samples.

Copolymer Melting Temperature vs Comonomer Incorporation. Figure 1 illustrates the correlations between polymer melting temperature and percent comonomer incorporation according to Table 1. For comparison, data reported by Graef et al. (**1**/MAO, $T_p = 20$ °C) are also plotted in Figure 1. For polymer samples produced by each catalyst at 0 °C, the relationship is fairly linear, with the melting temperature decreasing as larger percentages of comonomer are incorporated into the polymer. As observed by Graef et al., the identity of the comonomer employed has no coherent effect on the change in melting temperature.²⁷ The four best linear fits from Figure 1 are found to be

$$\text{1/MAO at } 20\text{ }^{\circ}\text{C: } T_m = 141.4\text{ }^{\circ}\text{C} - 13.8\text{ }^{\circ}\text{C}(\text{mol } \%$$
 comonomer)
with $R^2 = 0.850$

$$\text{1/MAO at } 0\text{ }^{\circ}\text{C: } T_m = 148.4\text{ }^{\circ}\text{C} - 9.5\text{ }^{\circ}\text{C}(\text{mol } \%$$
 comonomer)
with $R^2 = 0.959$

$$\text{2/MAO at } 0\text{ }^{\circ}\text{C: } T_m = 151.0\text{ }^{\circ}\text{C} - 8.0\text{ }^{\circ}\text{C}(\text{mol } \%$$
 comonomer)
with $R^2 = 0.919$

$$\text{3/MAO at } 0\text{ }^{\circ}\text{C: } T_m = 161.7\text{ }^{\circ}\text{C} - 7.6\text{ }^{\circ}\text{C}(\text{mol } \%$$
 comonomer)
with $R^2 = 0.953$

The highest copolymer melting temperature for any given branching content is provided by **3**/MAO. For this catalyst system, the best fit linear relationship suggests that each additional mol % of incorporated branches decreases the polymer melting temperature by ~ 7.6 °C.

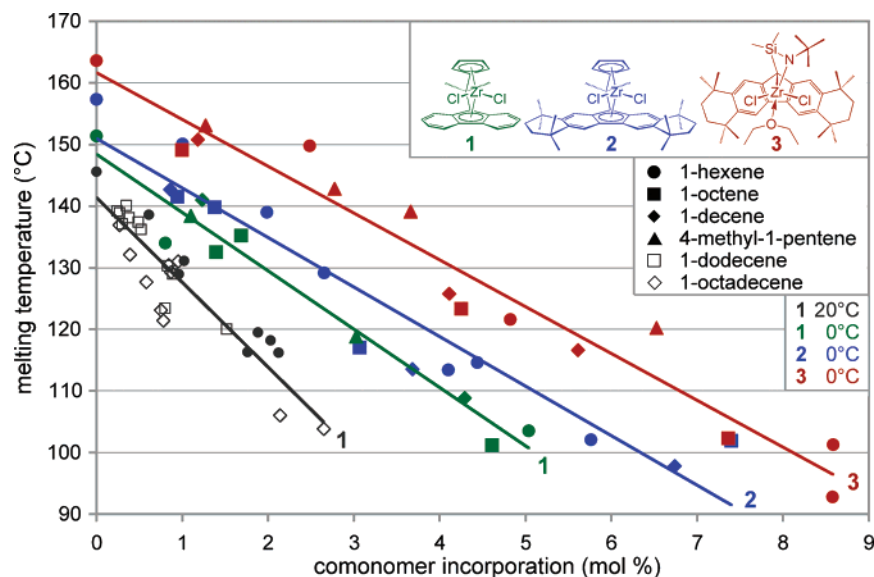


Figure 1. Copolymer melting temperature decreases with increasing comonomer incorporation for catalysts **1**, **2**, and **3** at polymerization temperatures of 0 °C. The gray line represents data reported by Graef et al. for catalyst **1** at a polymerization temperature of 20 °C.²⁷

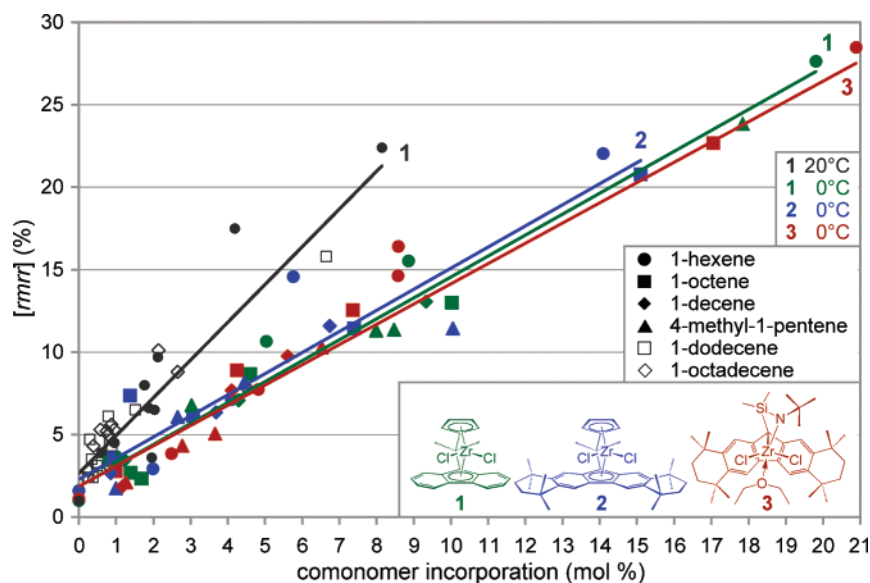


Figure 2. Fraction of site epimerization stereoregularity (*rmrr*) generally increases with increasing comonomer incorporation. The gray line represents data reported by Graef et al. for catalyst **1** at a polymerization temperature of 20 °C.²⁷

The melting temperatures of the *s*-PP homopolymers increase in the order **1** < **2** < **3** (151, 157, and 164 °C), and this relative ordering persists for their respective copolymers. Copolymers made with **1**/MAO at 0 °C containing more than 6% comonomer are generally amorphous and have a very weak, variable, or absent melting endotherm by DSC. Copolymers made with **1**/MAO at 0 °C containing less than 6% comonomer generally exhibit some crystallinity and a defined melting temperature. This breakpoint percentage is somewhat greater for **2**/MAO and **3**/MAO: 8% and 9%, respectively. Note that a copolymer produced with **3** having about 2% comonomer incorporation has the same melting temperature (ca. 150 °C) as the homopolymer produced by **1**. This implies that the stereoregularity alone produced by **1** disrupt crystallinity to the same extent as the stereoregularity and 2 mol % branching produced by **3**—consistent with the observation that **3**/MAO is highly syndiospecific.¹⁰

Stereoregularity vs Comonomer Incorporation. As noted above, the data from Graef and co-workers²⁷ can be plotted to show a rough linear correlation between site epimerization mistakes and comonomer incorporation with **1**/MAO operating

at 20 °C: %*rmrr* = 2.6 + 2.3(mol % comonomer) with $R^2 = 0.846$. With a lower polymerization temperature of 0 °C, the corresponding best linear fits for **1**, **2**, and **3**—as depicted in Figure 2—are

$$\text{1/MAO at 0 °C: \%[rmrr] = 1.8 + 1.3 (mol \% comonomer) with } R^2 = 0.973$$

$$\text{2/MAO at 0 °C: \%[rmrr] = 2.3 + 1.3 (mol \% comonomer) with } R^2 = 0.897$$

$$\text{3/MAO at 0 °C: \%[rmrr] = 1.8 + 1.2 (mol \% comonomer) with } R^2 = 0.928$$

and collectively for **1**, **2**, and **3**/MAO at 0 °C:

$$\%[rmrr] = 2.0 + 1.2 (mol \% comonomer) \text{ with } R^2 = 0.935$$

The important comparison is that at 0 °C each incorporated comonomer induces about half the number of single *m* mistakes (ca. 1.2) compared to **1**/MAO at 20 °C (ca. 2.3). As can be

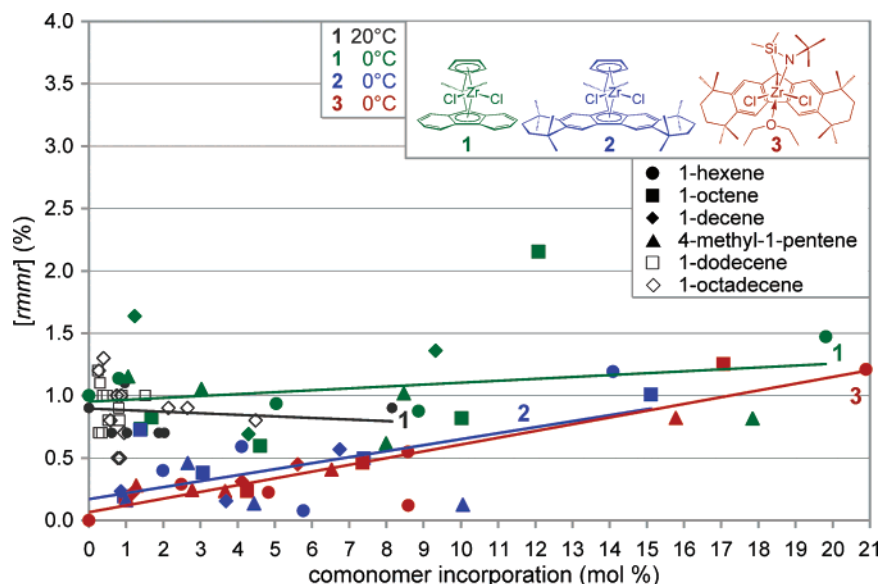


Figure 3. Fraction of enantiofacial misinsertion stereoerrors ($[rmmr]$) is weakly correlated to increasing comonomer incorporation. The gray line represents data reported by Graef et al. for catalyst **1** at a polymerization temperature of 20 °C.²⁷

seen from the similarity of the linear fits in Figure 2, the three catalysts provide a statistically similar number of $rmrr$ mistakes at 0 °C.

Figure 3 demonstrates that there is a slight correlation between % comonomer incorporation and the double m mistakes that arise from enantiofacial misinsertion ($rmmr$). Higher comonomer incorporation rates effect a small increase in this kind of stereoerror. A similar correlation cannot be identified in the data produced by Graef et al., perhaps because they did not form copolymers with more than about 8% comonomer incorporation.²⁷ One noteworthy observation is that the polymers produced by **2**/MAO and **3**/MAO at 0 °C have the lowest average $[rmmr]$ content, as might be anticipated on the basis of the high enantiofacial selectivity of these catalysts.^{7,10} The average $[rmmr]$ percentages for the copolymers with all reported comonomers are calculated below, categorized by catalyst and polymerization temperature:

1/MAO at 20 °C: $[rmmr]$ average = 0.9%²⁷

1/MAO at 0 °C: $[rmmr]$ average = 1.0%

2/MAO at 0 °C: $[rmmr]$ average = 0.4%

3/MAO at 0 °C: $[rmmr]$ average = 0.4%

Effective Action of Stereoerrors and Branches as Chain Disruptors. For the syndiotactic copolymers, there are three possible chain disruptions that can conceivably contribute to the melting point depression: side-chain branches, the $rmrr$ site epimerization stereoerror, and the $rmmr$ enantiofacial misinsertion stereoerror. Each of these should disrupt polymer crystallinity, whether the mode of action is to prevent neighboring chains from enjoying optimal van der Waals nonbonded interactions in the crystal lattice (branches) or to disrupt the conformational regularity of the polymer chain and thereby diminish its ability to participate in a crystallite (stereoerrors). Figure 4 plots the effect of these chain disruptions on polymer melting temperature as a function of their percent molar abundance. The red line (circles) corresponds to a series of s -PP homopolymers made with three different catalysts (**1**, **2**, and **3**) at four different temperatures (−15, 0, 25, and 90 °C).¹⁰ The relationship is quite linear ($R^2 = 0.956$) when the $rmrr$ (up to 7.8%) and $rmmr$ (up to 1.9%) stereoerrors are simply added

and counted as equally effective chain disruptors. The equation of this line is $T_m = 165.4\text{ °C} - 5.0\text{ °C (mol \% disruptions)}$ and provides a baseline for the inherent effect of stereoerrors on the melting temperature of syndiotactic homopolypropylene.

The blue line of Figure 4 (squares) corresponds to the copolymers of Table 1 and assumes that $rmrr$, $rmmr$, and branches are equally effective chain disruptors. As can be seen from its significant deviation from the homopolymer reference line, this assumption greatly overestimates the cumulative chain disruption ability of $rmrr$, $rmmr$, and branches. The green line of Figure 4 (triangles) corresponds to the copolymers of Table 1, counts the stereoerrors ($rmrr$ and $rmmr$) as chain disruptors, but *ignores the branches altogether*. Interestingly, this approach provides a very close match to the data obtained for the homopolymers. This near match suggests that $rmrr$, $rmmr$, and branches do not behave as independent chain disruptors. A reasonable interpretation is that these disruptors are not randomly distributed along the polymer backbone. In fact, the previously noted proportional increase of the site epimerization stereoerrors in response to comonomer incorporation ($\%[rmrr] = 2.0 + 1.2 \cdot (\% \text{ comonomer})$) suggests that branches and $rmrr$ are spatially correlated along the polymer backbone, which would not allow them to independently disrupt the chain. In essence, an incorporated higher α -olefin may momentarily slow propagation and allow for a subsequent site epimerization event, as long as the incorporated branch is in the vicinity of the transition metal. The effect would only be possible while the inserted comonomer branch is still in close proximity to the metal center—probably within a few monomer units of the metal. At 0 °C there is an average of 1.2 induced $rmrr$ mistakes per branch, and this approximate 1:1 correlation suggests that these chain disruptors are proximally located and operate as a single chain disrupting unit. This can explain the duplicative effect of the branches and the close match of the red and green lines of Figure 4.

The spatial correlation between branches and stereoerrors is further implicated upon dyad sequence analysis by ¹³C NMR. The relative integrations of the **PP**, **PC**, and **CC** dyad methylene peaks (**P** = propylene; **C** = comonomer) of the studied copolymer samples show that the monomer distributions are random, and so a statistical distribution of tetrad (**xPPx**, **xPCx**, **xCx**) or hexad (**xxPPxx**, **xxPCxx**, **xxCCxx**) peaks is expected for each. However, the higher-level sequence distributions

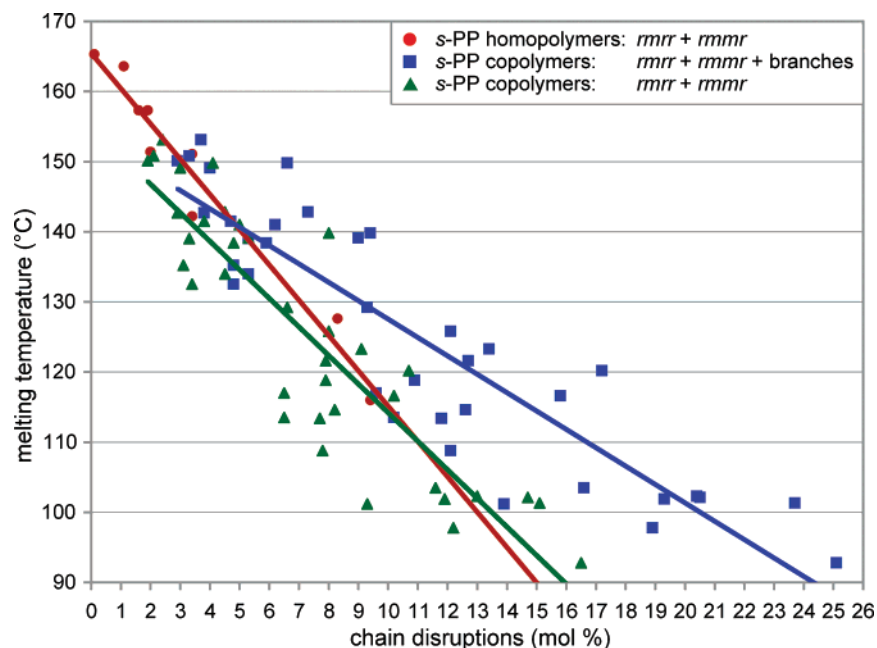


Figure 4. Counting the branches for *s*-PP copolymers as distinct chain disruptors overestimates their effect on copolymer melting temperature (squares). Ignoring the branches and assuming they operate in concert as a single chain disruptor with a *rmmr* stereoerror (triangles) provides a closer match to a series of *s*-PP homopolymers (circles).

observed by ^{13}C NMR do not correspond to the expected statistical distributions for monomer sequences, the expected stereosequences, or any combination thereof. This suggests that the higher-level sequence distributions are perturbed by non-statistical stereosequences in proximity to isolated branches in the polymer chain. In particular, stereoerrors are found to be more abundant in proximity to the branches.³⁵

Because of the branch/site epimerization correlation, the intrinsic effect of branches on crystallinity disruption can be understood even with a series of copolymers with significant *rmmr* stereoerrors. The important remaining consideration is enantiofacial misinsertion (*rmmr*). As long as the frequency of this mistake is low, the corresponding copolymers should provide useful information about the true effect of branches. Since the copolymers prepared by **3**/MAO have minimal *rmmr* mistakes (average = 0.4%; average = 0.3% when comonomer incorporation <9%), they serve as the best existing models for measuring the true effects of branching in syndiotactic polypropylene.

Conclusions

A series of syndiotactic propylene/higher α -olefin copolymers was prepared at 0 °C with the parent Ewen–Razavi catalyst (**1**), a sterically expanded Ewen–Razavi catalyst (**2**), and a sterically expanded constrained geometry catalyst (**3**). The catalyst system **3**/MAO provided the series of copolymers having the highest melting temperature for a given comonomer incorporation. The melting temperature depression was linearly dependent on the molar fraction of comonomer but was seemingly independent of the nature of the branch (isobutyl, *n*-butyl, *n*-hexyl, *n*-octyl): $T_m = 161.7\text{ °C} - 7.6\text{ °C}(\text{mol \% comonomer})$. At 0 °C, these three catalysts generated an average of 1.2 additional site epimerization stereoerrors (*rmmr*) for each comonomer incorporated. This approximate 1:1 correlation suggested that the α -olefin branch induced the competing unimolecular event and is, therefore, spatially proximal to the corresponding stereoerror along the polymer backbone. Thus, when plotting the polymer melting temperature vs the chain disruptor concentration, it was necessary to treat the branches

and their paired *rmmr* stereoerrors as a single chain disruptor in order to match the corresponding relationship found with syndiotactic polypropylene homopolymers. Thus, the intrinsic effect of branches on *s*-PP melting temperature is best understood with the copolymers having the fewest enantiofacial misinsertions (*rmmr* mistakes), and these are obtained with the sterically expanded constrained geometry catalyst, **3**/MAO. This catalyst system will facilitate future work on measurements of copolymer mechanical properties as a function of comonomer incorporation in syndiotactic polypropylene.

Experimental Section

General Considerations. Toluene was filtered through an mBraun solvent filtration system, degassed, and stored in a Straus flask until needed. Propylene from Scott Specialty Gases (>99.5%) was used following passage through a Matheson 6410 drying system equipped with an OXYSORB column. 4-Methyl-1-pentene (TCI, 97%), 1-hexene (ICN Biomedicals, 97%), 1-octene (MP Biomedicals, 99%), and 1-decene (Acros, 95%) were dried by stirring over CaH_2 and vacuum-transferred into Straus flasks to be stored until needed. MAO was acquired from Albemarle as a 30 wt % solution in toluene and was prepared by drying under high vacuum at 70 °C for 3 days to remove the solvent and residual trimethylaluminum. The solid MAO was stored under nitrogen in a glovebox and weighed out as needed.

^{13}C NMR spectra were recorded using an INOVA 300 spectrometer observing at 75.4 MHz with at least 2000 transients collected using a 70° pulse, 3 s acquisition time, and 2.5 s d_1 delay. The temperature was held constant at 100 °C. (Some samples required different temperatures between 90 and 110 °C to achieve optimum homogeneity.) Polymer samples for NMR characterization were prepared by dissolving ~100 mg of polymer in ~1.5 mL of 1,1,2,2-tetrachloroethane- d_2 . Chemical shifts were referenced to the center peak of the $\text{C}_2\text{D}_2\text{Cl}_4$ solvent triplet at 74.3 ppm. Peak assignments followed those of Busico³⁶ (propylene pentads) and Asakura³⁷ (α -olefin peaks). Integration of the resolved peaks in the methyl region (19.7–22.0 ppm) was used to determine the pentad distribution.

Polymer melting temperatures were determined using a TA Instruments Q600 SDT differential scanning calorimeter under an argon purge at a heating rate of 10 °C/min from 25 to 180 °C. The

melting temperature was taken as the maximum of the melting endotherm on the second heating cycle.

Catalysts **1–3** were prepared according to literature procedures.^{7,8} Stock solutions of each catalyst were prepared by placing 0.100 g of **1**, 0.200 g of **2**, and 0.250 g of **3** into separate 100 mL volumetric flasks and dissolving in toluene. The solutions thus prepared had the following concentrations: [**1**] = 2.31×10^{-3} M, [**2**] = 3.00×10^{-3} M, and [**3**] = 3.33×10^{-3} M. To initiate each polymerization, 1.0 mL of the appropriate catalyst stock solution was injected into the polymerization reactor (vide infra).

General Polymerization Procedure. CAUTION: All polymerizations should be carried out in a fume hood behind a blast shield. Polymerizations were carried out in an 85 mL glass Lab-Crest (Andrews Glass Co.) cylindrical polymerization reactor equipped with a 2.5×0.375 in. octagonal stir bar to provide surface agitation while stirring. The apparatus was pumped into the glovebox where solid MAO (1000 equiv) and an appropriate amount of the selected liquid comonomer were added. The reactor was sealed, removed from the box, and purged with propylene for 3 min before being resealed and cooled to 0 °C. Propylene was condensed into the reactor to a total volume of ~25 mL, and the system was equilibrated at 0 °C for 10 min, after which 1.0 mL of the appropriate catalyst stock solution was injected using a 5 mL Hamilton gastight syringe. After polymerizing for 2 min³⁸ at 0 °C, the polymerization was quenched by injection of 5 mL of a 10% (v/v) solution of concentrated aqueous HCl in methanol. The reaction solution was poured into an additional 200 mL of acidic methanol and stirred vigorously. The polymer was collected by filtration and thrice washed with fresh methanol before being dried in vacuo.

Acknowledgment. This research was supported by grants from The Robert A. Welch Foundation (No. A-1537) and the Texas Advanced Technology Program (No. 010366-0196-2003). The National Science Foundation (CAREER CHE-0548197) is also graciously acknowledged for financial support.

Supporting Information Available: Additional polymer characterization data, representative NMR spectra, DSC thermograms, and a detailed analysis of monomer sequences. This material is available free of charge via the Internet at <http://pubs.acs.org>.

References and Notes

- Ewen, J. A.; Jones, R. L.; Razavi, A.; Ferrara, J. D. *J. Am. Chem. Soc.* **1988**, *110*, 6255–6256.
- Private communication with A. Razavi of Total Petrochemicals, Nov 17, 2005.
- Shamshoum, E.; Schardl, J. In *Metallocene-Catalyzed Polymers: Materials Properties, Processing and Markets*; Benedikt, G. M., Goodall, B. L., Eds.; Plastics Design Library: Norwich, NY, 1998; pp 359–368.
- Nakamura, S. *Catal. Surv. Jpn.* **1998**, *2*, 107–112.
- (a) Herzog, T. A.; Zubris, D. L.; Bercaw, J. E. *J. Am. Chem. Soc.* **1996**, *118*, 11988–11989. (b) Miyake, S.; Bercaw, J. E. *J. Mol. Catal. A: Chem.* **1998**, *128*, 29–39. (c) Veghini, D.; Henling, L. M.; Burkhardt, T. J.; Bercaw, J. E. *J. Am. Chem. Soc.* **1999**, *121*, 564–573. (d) Zubris, D. L.; Veghini, D.; Herzog, T. A.; Bercaw, J. E. In *Olefin Polymerization*; Arjunan, P., McGrath, J. E., Hanlon, T. L., Eds.; ACS Symposium Series 749; American Chemical Society: Washington, DC, 2000; pp 2–14.
- (a) Tian, J.; Hustad, P. D.; Coates, G. W. *J. Am. Chem. Soc.* **2001**, *123*, 5134–5135. (b) Mitani, M.; Furuyama, R.; Mohri, J.; Saito, J.; Ishii, S.; Terao, H.; Kashiwa, N.; Fujita, T. *J. Am. Chem. Soc.* **2002**, *124*, 7888–7889. (c) Makio, H.; Kashiwa, N.; Fujita, T. *Adv. Synth. Catal.* **2002**, *344*, 477–493.
- Miller, S. A.; Bercaw, J. E. *Organometallics* **2004**, *23*, 1777–1789.
- Irwin, L. J.; Reibenspies, J. H.; Miller, S. A. *J. Am. Chem. Soc.* **2004**, *126*, 16716–16717.
- Irwin, L. J.; Reibenspies, J. H.; Miller, S. A. *Polyhedron* **2005**, *24*, 1314–1324.
- Irwin, L. J.; Miller, S. A. *J. Am. Chem. Soc.* **2005**, *127*, 9972–9973.
- Simpson, D. M.; Vaughan, G. A. In *Encyclopedia of Polymer Science and Technology*; Mark, H. F., Ed.; John Wiley & Sons: New York, 2003; Vol. 2, pp 441–482.
- (a) Tait, P. J. T.; Berry, I. G. In *Comprehensive Polymer Science*; Eastmond, G. C., Ledwith, A., Russo, S., Sigwalt, P., Eds.; Pergamon Press: Oxford, 1989; Vol. 4, pp 575–584. (b) Chadwick, J. C. In *Encyclopedia of Polymer Science and Technology*; Mark, H. F., Ed.; John Wiley & Sons: New York, 2003; Vol. 8, pp 517–536.
- (a) Stevens, J. C.; Timmers, F. J.; Wilson, D. R.; Schmidt, G. F.; Nickias, P. N.; Rosen, R. K.; Knight, G. W.; Lai, S. Y. Eur. Patent Appl. EP 416815-A2, 1991 (Dow Chem. Co.). (b) Canich, J. M. Eur. Patent Appl. EP 420436-A1, 1991 (Exxon Chem. Co.). (c) McKnight, A. L.; Waymouth, R. M. *Chem. Rev.* **1998**, *98*, 2587–2598. (d) Leino, R. In *Encyclopedia of Polymer Science and Technology*; Mark, H. F., Ed.; John Wiley & Sons: New York, 2003; Vol. 4, pp 136–179. (e) Wasserman, E. P. In *Encyclopedia of Polymer Science and Technology*; Mark, H. F., Ed.; John Wiley & Sons: New York, 2003; Vol. 7, pp 35–103.
- Chemical Week Associates “PP market moves into balance”. *Chem. Week* **2003**, Aug 13, 26–27.
- Lieberman, R.; Stewart, C. In *Encyclopedia of Polymer Science and Technology*; Mark, H. F., Ed.; John Wiley & Sons: New York, 2003; Vol. 11, pp 287–358.
- De Rosa, C.; Auriemma, F. *J. Am. Chem. Soc.* **2006**, *128*, 11024–11025.
- Brintzinger, H.-H.; Fisher, D.; Mülhaupt, R.; Rieger, B.; Waymouth, R. M. *Angew. Chem., Int. Ed. Engl.* **1995**, *34*, 1143–1170.
- Resconi, L.; Cavallo, L.; Fait, A.; Piemontesi, F. *Chem. Rev.* **2000**, *100*, 1253–1345.
- De Rosa, C.; Auriemma, F.; Di Capua, A.; Resconi, L.; Guidotti, S.; Camurati, I.; Nifant'ev, I. E.; Laishevstev, I. P. *J. Am. Chem. Soc.* **2004**, *126*, 17040–17049.
- Poon, B.; Rogunova, M.; Hiltner, A.; Baer, E.; Chum, S. P.; Galeski, A.; Piorkowska, E. *Macromolecules* **2005**, *38*, 1232–1243.
- De Rosa, C.; Dello Iacono, S.; Auriemma, F.; Ciaccia, E.; Resconi, L. *Macromolecules* **2006**, *39*, 6098–6109.
- Lotz, B.; Ruan, J.; Thierry, A.; Alfonso, G. C.; Hiltner, A.; Baer, E.; Piorkowska, E.; Galeski, A. *Macromolecules* **2006**, *39*, 5777–5781.
- Naga, N.; Mizunuma, K.; Sadatoshi, H.; Kakugo, M. *Macromolecules* **1997**, *30*, 2197–2200.
- De Rosa, C.; Talarico, G.; Caporaso, L.; Auriemma, F.; Galimberti, M.; Fusco, O. *Macromolecules* **1998**, *31*, 9109–9115.
- De Rosa, C.; Auriemma, F.; Orlando, I.; Talarico, G.; Caporaso, L. *Macromolecules* **2001**, *34*, 1663–1672.
- Naga, N.; Mizunuma, K.; Sadatoshi, H.; Kakugo, M. *Polymer* **2000**, *41*, 203–209.
- Graef, S. M.; Wahner, U. M.; Van Reenen, A. J.; Brull, R.; Sanderson, R. D.; Pasch, H. *J. Polym. Sci., Part A* **2002**, *40*, 128–140.
- Quijada, R.; Guevara, J. L.; Galland, G. B.; Rabagliati, F. M.; Lopez-Majada, J. M. *Polymer* **2005**, *46*, 1567–1574.
- Jüngling, S.; Mülhaupt, R.; Fischer, D.; Langhauser, F. *Angew. Makromol. Chem.* **1995**, *229*, 93–112.
- Thomann, R.; Kressler, J.; Mülhaupt, R. *Polymer* **1998**, *39*, 1907–1915.
- Hauser, G.; Schmidtke, J.; Strobl, G. *Macromolecules* **1998**, *31*, 6250–6258.
- Heck, B.; Hugel, T.; Iijima, M.; Strobl, G. *Polymer* **2000**, *41*, 8839–8848.
- (a) Nele, M.; Mohammed, M.; Xin, S.; Collins, S.; Dias, M. L.; Pinto, J. C. *Macromolecules* **2001**, *34*, 3830–3841. (b) Mohammed, M.; Nele, M.; Al-Humydi, A.; Xin, S.; Stapleton, R. A.; Collins, S. *J. Am. Chem. Soc.* **2003**, *125*, 7930–7941.
- Miller, S. A.; Bercaw, J. E. *Organometallics* **2006**, *25*, 3576–3592.
- See the Supporting Information for detailed spectra and analysis.
- Busico, V.; Cipullo, R.; Monaco, G.; Vacatello, M. *Macromolecules* **1997**, *30*, 6251–6263.
- Asakura, T.; Demura, M.; Nishiyama, Y. *Macromolecules* **1991**, *24*, 2334–2340.
- Some polymerizations were allowed to run longer; the times are indicated in Table 1.

MA070060Q